

Article

The Effect of the Vadasz Number on the Onset of Thermal Convection in Rotating Bidisperse Porous Media

Florinda Capone  and Roberta De Luca * 

Department of Mathematics and Applications “Renato Caccioppoli”, University of Naples Federico II, Via Cinzia, 80126 Naples, Italy; fcapone@unina.it

* Correspondence: roberta.deluca@unina.it

Received: 19 June 2020; Accepted: 3 October 2020; Published: 6 October 2020



Abstract: The onset of thermal convection in uniformly rotating bidisperse horizontal porous layer, uniformly heated from below, is analyzed. A generalized Darcy equation for the macro-phase is considered to take the Vadasz number into account. It is proved that the presence of the Vadasz number can give rise to oscillatory motion at the loss of stability of thermal conduction solution.

Keywords: bidisperse porous medium; convection; inertia effect; thermal rotating convection

1. Introduction

The onset of thermal convection is a very active research field due to the numerous applications in real world phenomena (see, for example, [1–3] and references therein). Recently, a great attention has been played to bidisperse porous media. A bidisperse porous medium is composed by clusters of large particles that are agglomerations of small particles that can be looked as a porous medium in which fractures or tunnels are introduced (see [4–6]). Denoting by Φ and ε the porosity associated with the macro pores between the clusters and the porosity of the micro pores within the clusters, respectively, the fraction of volume occupied by the micro pores is $\varepsilon(1 - \Phi)$ while the solid skeleton occupies the fraction of volume $(1 - \varepsilon)(1 - \Phi)$. Bidisperse porous media may be artificial [6] and they are involved in many real engineering processes and geophysical applications, such as, for example, in thermal convection in heat pipes [7], in the theory of landslides [8], as catalyst in the production of high octane petrol [9].

Recently, in [10], the effect of Vadasz number on thermohaline convection in a horizontal bidisperse layer, has been investigated. In particular, the destabilizing effect of heating from below opposite to the stabilizing effect of the layer salted from below is studied. The effect of Vadasz number has been widely studied for a single porosity medium [11–19], together with other effects, such as the influence of an external magnetic field acting on an electrically conducting fluid [15] and the presence of a chemical dissolved in the fluid [16]. In these models, a generalized Darcy equation is employed to include the time derivative term, multiplied by a positive constant, of the seepage velocity. In [18], Vadasz pointed out that the inertia term has a strong effect on the onset of convection in a rotating porous layer. The uniform rotation in porous media finds relevant applications in the food process industry, in geophysics, and in the chemical industry dealing with rotating machinery. For this reason, many papers are devoted to the onset of thermal convection in rotating porous media (see, for example, [20–26] and references therein). As it is well known, convection can be named steady or oscillatory according to the secondary motion, arising when the initial rest state loses its stability, is steady or oscillatory. The transition from the steady rest state to an oscillatory solution (i.e., the onset of oscillatory convection) captures the interest of many researchers, because it is “less continuous”

with respect to the onset of steady convection and because the oscillatory convection is used in various fields that involve industrial and geophysical processes. Recently, in [27], the Coriolis effect has been analyzed in bidisperse porous layers showing that the thermal convection can only arise via a steady state (i.e., the principle of exchange of stability holds).

In this paper we reconsider the problem analyzed in [27], and investigate the effect of inertia in a rotating bidisperse porous medium. We consider the inertia term in the macro-phase only (since inertia effect can be neglected in the micro-phase) and show that inertia allows oscillatory convection at the instability threshold, as done in [10]. The plan of the paper is as follows. Section 2 is devoted to the introduction of mathematical model. To this aim, we consider the generalized Darcy equation for the macro-phase only [10] and assume the same temperature in the macro and micro pores [28]. The linear instability is performed in Section 3. In particular, Sections 3.1 and 3.2 are respectively devoted to the determination of the critical Rayleigh number for the onset of steady and oscillatory convection, where the steady or oscillatory convection respectively means that—when the rest state loses its stability—the convection arises via a steady or via an oscillatory (in time) state. In Section 4 the behaviour of the Rayleigh number for the onset of oscillatory convection with respect to the Taylor number and the acceleration coefficients is numerically investigated. The paper ends with a conclusion section in which the obtained results are summarized.

2. Preliminaries

Let us consider a homogeneous incompressible fluid filling a horizontal bidisperse porous layer L of depth d , uniformly heated from below and rotating about a vertical axis. Let us introduce $Oxyz$, which is an orthogonal frame of reference with fundamental unit vectors $\mathbf{i}, \mathbf{j}, \mathbf{k}$ (\mathbf{k} pointing vertically upwards) and denote by $\boldsymbol{\Omega} = \Omega\mathbf{k}$ the constant angular velocity of L . The aim of this paper is to investigate the influence of inertia effect on the onset of convection in bidisperse rotating porous medium, but considering the effect of a non-zero inertia term in the macro fluid velocity equation. In such a way, we restrict our attention to the more mathematically difficult, but contemporarily more physically interesting, case: in the analyzed situation, the heating wishes to destabilize the layer and initiate convective overturning, whereas the rotation of the layer acts in the opposite manner and it is stabilizing. The inertia term will be seen to have a very strong effect on the convection thresholds and we believe this is a justification for the analysis. When the inertial term is taken into account in the momentum equation of the macro-phase, the fluid motion is governed by the equations ([6,10,27])

$$\left\{ \begin{array}{l} \rho_0 c_a \mathbf{U}^f_{,t} = -\frac{\mu}{k_f} \mathbf{U}^f - \delta(\mathbf{U}^f - \mathbf{U}^p) - \nabla p^f + \rho_0 g \alpha T \mathbf{k} - \frac{2\rho_0 \Omega}{\Phi} \mathbf{k} \times \mathbf{U}^f, \\ -\frac{\mu}{k_p} \mathbf{U}^p - \delta(\mathbf{U}^p - \mathbf{U}^f) - \nabla p^p + \rho_0 g \alpha T \mathbf{k} - \frac{2\rho_0 \Omega}{\varepsilon} \mathbf{k} \times \mathbf{U}^p = \mathbf{0}, \\ (\rho c)_m T_{,t} + (\rho c)_f (\mathbf{U}^f + \mathbf{U}^p) \cdot \nabla T = k_m \Delta T, \\ \nabla \cdot \mathbf{U}^f = 0, \quad \nabla \cdot \mathbf{U}^p = 0, \end{array} \right. \tag{1}$$

with

$$\begin{aligned} p^s &= P^s - \frac{\rho_0}{2} |\boldsymbol{\Omega} \mathbf{k} \times \mathbf{x}|^2 \\ (\rho c)_m &= (1 - \Phi)(1 - \varepsilon)(\rho c)_s + \Phi(\rho c)_f + \varepsilon(1 - \Phi)(\rho c)_p \\ k_m &= (1 - \Phi)(1 - \varepsilon)k_s + \Phi k_f + \varepsilon(1 - \Phi)k_p \end{aligned}$$

and \mathbf{U}^s is the seepage velocity, T is the temperature, P^s is the pressure, c_a is the acceleration coefficient, δ is the interaction coefficient, $\mathbf{g} = -g\mathbf{k}$ is the gravity, $\mathbf{x} = (x, y, z)$, μ is the fluid viscosity, ρ_0 is the reference (constant) density, k_r is the permeability, α is the thermal expansion coefficient, c is the

specific heat, c_p is the specific heat at a constant pressure, and k_m is the thermal conductivity. Moreover, $(\cdot)_{,t}$ denotes the partial derivative with respect to t and $s = \{f, p\}$ being the subscript f and p referring to the macro and micro pore effects. To (1), we append the boundary conditions

$$T(x, y, 0, t) = T_L, \quad T(x, y, d, t) = T_U, \quad T_L > T_U, \tag{2}$$

$$\mathbf{U}^s \cdot \mathbf{n} = 0, \text{ on } z = 0, d, \quad s = \{f, p\},$$

being \mathbf{n} the unit vector in the upward vertical direction. Model (1)–(2) admits the thermal conduction solution

$$\mathbf{U}_b^f = \mathbf{0}, \quad \mathbf{U}_b^p = \mathbf{0}, \quad T_b = -\beta z + T_L, \quad \beta = \frac{T_L - T_U}{d}. \tag{3}$$

Introducing the perturbation fields

$$\mathbf{u}^s = \mathbf{U}^s - \mathbf{U}_b^s, \quad \pi^s = P^s - p_b, \quad \theta = T - T_b, \quad s = \{f, p\} \tag{4}$$

setting

$$\begin{cases} \mathbf{x} = d\mathbf{x}_*, & t = \mathcal{I}t_*, & \theta = \theta_* T^\sharp, & \mathbf{u}^s = U\mathbf{u}_*^s, & \pi^s = P\pi_*^s, & s = \{f, p\}, \\ \mathcal{I} = \frac{(\rho c)_m d^2}{k_m}, & U = \frac{k_m}{(\rho c)_f d'}, & T^\sharp = \beta d, & P = \frac{k_m \mu}{k_f (\rho c)_f} \end{cases} \tag{5}$$

the non-dimensional system (omitting the asterisks) governing the evolution of perturbation fields is

$$\begin{cases} -J\mathbf{u}_{,t}^f - \mathbf{u}^f - \gamma(\mathbf{u}^f - \mathbf{u}^p) - \nabla \pi^f + R\theta\mathbf{k} - \mathcal{T}\mathbf{k} \times \mathbf{u}^f = \mathbf{0}, \\ -k_r \mathbf{u}^p - \gamma(\mathbf{u}^p - \mathbf{u}^f) - \nabla \pi^p + R\theta\mathbf{k} - \eta\mathcal{T}\mathbf{k} \times \mathbf{u}^p = \mathbf{0}, \\ \theta_{,t} + (\mathbf{u}^f + \mathbf{u}^p) \cdot \nabla \theta = w^f + w^p + \Delta \theta, \\ \nabla \cdot \mathbf{u}^f = 0, \quad \nabla \cdot \mathbf{u}^p = 0, \end{cases} \tag{6}$$

with $\mathbf{u}^f = (u^f, v^f, w^f)$, $\mathbf{u}^p = (u^p, v^p, w^p)$ and

$$\begin{cases} J = \frac{\rho_0 c_a k_f k_m}{(\rho c)_m \mu d^2} = \text{Vadasz number}, \\ \gamma = \frac{\delta k_f}{\mu}, \quad \mathcal{T} = \frac{2\rho_0 \Omega k_f}{\mu \Phi} = \text{Taylor number}, \quad k_r = \frac{k_f}{k_p}, \quad \eta = \frac{\Phi}{\varepsilon}, \\ R = \frac{\rho_0 \alpha g \beta d^2 k_f (\rho c)_f}{\mu k_m} = \text{Rayleigh thermal number}. \end{cases} \tag{7}$$

To (6) we append smooth initial data

$$\mathbf{u}^s(\mathbf{x}, 0) = \mathbf{u}_0^s(\mathbf{x}); \quad \pi^s(\mathbf{x}, 0) = \pi_0^s(\mathbf{x}); \quad \theta(\mathbf{x}, 0) = \theta_0(\mathbf{x}) \tag{8}$$

with $\nabla \cdot \mathbf{u}_0^s = 0, s = \{f, p\}$ and the boundary conditions

$$w^f = w^p = \theta = 0, \quad \text{on } z = 0, 1. \tag{9}$$

In the sequel, we perform the linear stability analysis of the null solution of (6)–(9) under the assumption that the perturbations $\{u^s, v^s, w^s, \pi^s, \theta\}$ ($s = \{f, p\}$) are periodic in the horizontal directions x and y , respectively, of period $2\pi/a_x, 2\pi/a_y$ and denote by

$$V = \left[0, \frac{2\pi}{a_x}\right] \times \left[0, \frac{2\pi}{a_y}\right] \times [0, 1]$$

the periodicity cell.

3. Linear Instability

Neglecting the nonlinear terms, (6) reduces to

$$\begin{cases} -J\mathbf{u}_t^f - \mathbf{u}^f - \gamma(\mathbf{u}^f - \mathbf{u}^p) - \nabla\pi^f + R\theta\mathbf{k} - \mathcal{T}\mathbf{k} \times \mathbf{u}^f = \mathbf{0}, \\ -k_r\mathbf{u}^p - \gamma(\mathbf{u}^p - \mathbf{u}^f) - \nabla\pi^p + R\theta\mathbf{k} - \eta\mathcal{T}\mathbf{k} \times \mathbf{u}^p = \mathbf{0}, \\ \theta_{,t} = w^f + w^p + \Delta\theta, \\ \nabla \cdot \mathbf{u}^f = 0, \quad \nabla \cdot \mathbf{u}^p = 0, \end{cases} \tag{10}$$

under the boundary conditions (9). Setting

$$\zeta^s = (\nabla \times \mathbf{u}^s) \cdot \mathbf{k}, \quad s = \{f, p\}, \tag{11}$$

the third components of the curl of (10)₁ and (10)₂, respectively, lead to the following equations:

$$\begin{cases} J\zeta_{,t}^f + \zeta^f + \gamma(\zeta^f - \zeta^p) - \mathcal{T}w_{,z}^f = 0, \\ k_r\zeta^p + \gamma(\zeta^p - \zeta^f) - \eta\mathcal{T}w_{,z}^p = 0. \end{cases} \tag{12}$$

Since the system (10) is autonomous, setting $\forall \varphi \in \{u^s, v^s, w^s, \pi^s, \theta\}$

$$\varphi(x, y, z, t) = \tilde{\varphi}(x, y, z)e^{\sigma t} \tag{13}$$

with $\sigma \in \mathbb{C}$ and substituting, respectively, in (12)₁ and in (12)₂, one has that:

$$\begin{cases} (J\sigma + 1 + \gamma)\zeta^f - \gamma\zeta^p - \mathcal{T}w_{,z}^f = 0, \\ (\gamma + k_r)\zeta^p - \gamma\zeta^f - \eta\mathcal{T}w_{,z}^p = 0, \end{cases} \tag{14}$$

i.e.,

$$\begin{cases} \zeta^f = \frac{\mathcal{T}(\gamma + k_r)}{A}w_{,z}^f + \frac{\eta\gamma\mathcal{T}}{A}w_{,z}^p, \\ \zeta^p = \frac{\eta\mathcal{T}(1 + \sigma J + \gamma)}{A}w_{,z}^p + \frac{\gamma\mathcal{T}}{A}w_{,z}^f, \end{cases} \tag{15}$$

being

$$A = (\gamma + k_r)(1 + \sigma J) + \gamma k_r. \tag{16}$$

The third components of the double curl of (10)₁–(12)₂ are, respectively

$$\begin{cases} (1 + \sigma J + \gamma)\Delta w^f - \gamma\Delta w^p - R\Delta_1\theta + \mathcal{T}\zeta_{,z}^f = 0, \\ -\gamma\Delta w^f + (\gamma + k_r)\Delta w^p - R\Delta_1\theta + \eta\mathcal{T}\zeta_{,z}^p = 0, \end{cases} \tag{17}$$

with

$$\Delta_1 = \frac{\partial^2}{\partial x^2} + \frac{\partial^2}{\partial y^2}, \quad \Delta = \Delta_1 + \frac{\partial^2}{\partial z^2}.$$

The derivative with respect to z of (15)₁ and (15)₂ leads to:

$$\begin{cases} \zeta_{,z}^f = \frac{\mathcal{T}(\gamma + k_r)}{A}w_{,zz}^f + \frac{\eta\gamma\mathcal{T}}{A}w_{,zz}^p, \\ \zeta_{,z}^p = \frac{\gamma\mathcal{T}}{A}w_{,zz}^f + \frac{\eta\mathcal{T}(1 + \sigma J + \gamma)}{A}w_{,zz}^p \end{cases} \tag{18}$$

and substituting (18) into (17), one has that

$$\begin{cases} (1 + \sigma J + \gamma)\Delta w^f - \gamma\Delta w^p - R\Delta_1\theta + \mathcal{T}^2 \left[\frac{\gamma + k_r}{A}w_{,zz}^f + \frac{\eta\gamma}{A}w_{,zz}^p \right], \\ -\gamma\Delta w^f + (\gamma + k_r)\Delta w^p - R\Delta_1\theta + \eta\mathcal{T}^2 \left[\frac{\gamma}{A}w_{,zz}^f + \frac{\eta(1 + \sigma J + \gamma)}{A}w_{,zz}^p \right]. \end{cases} \tag{19}$$

On taking into account (19) and (10)₃–(10)₅, let us consider the following initial-boundary value problem

$$\begin{cases} (1 + \sigma J + \gamma)\Delta w^f - \gamma\Delta w^p - R\Delta_1\theta + \mathcal{T}^2 \left[\frac{\gamma + k_r}{A}w_{,zz}^f + \frac{\eta\gamma}{A}w_{,zz}^p \right], \\ -\gamma\Delta w^f + (\gamma + k_r)\Delta w^p - R\Delta_1\theta + \eta\mathcal{T}^2 \left[\frac{\gamma}{A}w_{,zz}^f + \frac{\eta(1 + \sigma J + \gamma)}{A}w_{,zz}^p \right], \\ \sigma\theta = w^f + w^p + \Delta\theta, \\ \nabla \cdot \mathbf{u}^f = 0, \quad \nabla \cdot \mathbf{u}^p = 0, \end{cases} \tag{20}$$

$$\mathbf{u}^s(\mathbf{x}, 0) = \mathbf{u}_0^s(\mathbf{x}); \quad \pi^s(\mathbf{x}, 0) = \pi_0^s(\mathbf{x}); \quad \theta(\mathbf{x}, 0) = \theta_0(\mathbf{x}) \tag{21}$$

$$w^f = w^p = \theta = 0, \quad \text{on } z = 0, 1 \tag{22}$$

and let us look for normal modes solutions, i.e.,:

$$\varphi(x, y, z, t) = \tilde{\varphi}(z)e^{i(a_x x + a_y y) + \sigma t}, \quad \forall \varphi \in \{w^f, w^p, \theta\}. \tag{23}$$

Setting $D = \frac{d}{dz}$, $a^2 = a_x^2 + a_y^2$, it follows that

$$\Delta_1\varphi = -a^2\varphi, \quad \Delta\varphi = (D^2 - a^2)\varphi, \quad \forall \varphi \in \{w^f, w^p, \theta\}. \tag{24}$$

Then, by virtue of (23) and (24), (20)₁–(20)₃ can be written as

$$\begin{cases} (1 + \sigma J + \gamma)(D^2 - a^2)\tilde{w}^f - \gamma(D^2 - a^2)\tilde{w}^p + Ra^2\tilde{\theta} + \frac{\mathcal{T}^2}{A} [(\gamma + k_r)D^2\tilde{w}^f + \eta\gamma D^2\tilde{w}^p] = 0, \\ -\gamma(D^2 - a^2)\tilde{w}^f + (\gamma + k_r)(D^2 - a^2)\tilde{w}^p + Ra^2\tilde{\theta} + \frac{\eta\mathcal{T}^2}{A} [\gamma D^2\tilde{w}^f + \eta(1 + \sigma J + \gamma)D^2\tilde{w}^p] = 0, \\ \sigma\tilde{\theta} = \tilde{w}^f + \tilde{w}^p + (D^2 - a^2)\tilde{\theta}. \end{cases} \quad (25)$$

In view of the boundary conditions, since the set $\{\sin n\pi z\}_{n \in \mathbb{N}}$ is a complete orthogonal system for $L^2(0, 1)$, $\forall \tilde{\varphi}(z) \in \{\tilde{w}^f, \tilde{w}^p, \tilde{\theta}\}$ there exists a sequence $\{\tilde{\varphi}_n(z)\}_{n \in \mathbb{N}}$ such that $\tilde{\varphi}(z) = \sum_{n=1}^{\infty} \tilde{\varphi}_n \sin n\pi z$.

Subsequently, setting $\Lambda_n = a^2 + n^2\pi^2$, (25) becomes

$$\begin{cases} -\left[\Lambda_n(1 + \sigma J + \gamma) + \frac{n^2\pi^2\mathcal{T}^2(\gamma + k_r)}{A}\right]w_0^f + \left(\Lambda_n\gamma - \frac{n^2\pi^2\mathcal{T}^2\eta\gamma}{A}\right)w_0^p + Ra^2\theta_0 = 0, \\ \left(\gamma\Lambda_n - \frac{n^2\pi^2\mathcal{T}^2\eta\gamma}{A}\right)w_0^f - \left[\Lambda_n(\gamma + k_r) + \frac{n^2\pi^2\mathcal{T}^2\eta^2(1 + \sigma J + \gamma)}{A}\right]w_0^p + Ra^2\theta_0 = 0, \\ w_0^f + w_0^p - (\Lambda_n + \sigma)\theta_0 = 0. \end{cases} \quad (26)$$

From (26), the condition guaranteeing the existence of a non null solution is the following

$$R = \frac{\Lambda_n + \sigma}{a^2} \frac{\Lambda_n^2 A^2 + n^2 \pi^2 \mathcal{T}^2 \Lambda_n B + n^4 \pi^4 \mathcal{T}^4 \eta^2}{\Lambda_n A C + n^2 \pi^2 \mathcal{T}^2 E}, \quad (27)$$

being

$$B = (1 + \sigma J + \gamma)^2 \eta^2 + (\gamma + k_r)^2 + 2\eta\gamma^2, \quad (28)$$

$$C = 4\gamma + k_r + 1 + \sigma J, \quad E = \gamma(\eta - 1)^2 + \eta^2(1 + \sigma J) + k_r.$$

As it is well known, the onset of convection occurs or via a steady state—associated to $\sigma = 0$ —and named “steady convection”, or via an oscillatory state—associated to $\sigma = \pm i\sigma_1$ with $\sigma_1 \in \mathbb{R}^+ \setminus \{0\}$ —and named “oscillatory convection”. In the sequel, we determine the critical Rayleigh thermal number for the onset of steady and oscillatory convection.

3.1. Steady Convection

In order to determine the critical Rayleigh thermal number for the onset of steady convection, say R_S , we substitute $\sigma = 0$ in (27). Then

$$R_S = \min_{(n, a^2) \in \mathbb{N} \times \mathbb{R}^+} \frac{\Lambda_n}{a^2} \frac{\Lambda_n^2 A_1^2 + \pi^2 \mathcal{T}^2 \Lambda_n B_1 + n^4 \eta^2 \pi^4 \mathcal{T}^4}{\Lambda_n A_1 C_1 + n^2 \pi^2 \mathcal{T}^2 E_1}, \quad (29)$$

with A_1, B_1, C_1, E_1 given by (16), (28) when $\sigma = 0$, i.e.,

$$A_1 = \gamma + k_r + \gamma k_r, \quad B_1 = (1 + \gamma)^2 \eta^2 + (k_r + \gamma)^2 + 2\eta\gamma^2, \quad C_1 = 4\gamma + k_r + 1, \quad E_1 = \gamma(\eta - 1)^2 + \eta^2 + k_r. \quad (30)$$

The minimum with respect to $n \in \mathbb{N}$ of the right-hand side of (29) is attained at $n = 1$. Then, setting $\Lambda = \Lambda_1 = a^2 + \pi^2$, one has that

$$R_S = \min_{a^2 \in \mathbb{R}^+} f_s(a^2) := \min_{a^2 \in \mathbb{R}^+} \frac{\Lambda^2 A_1^2 + \pi^2 \mathcal{T}^2 \Lambda B_1 + \eta^2 \pi^4 \mathcal{T}^4}{\Lambda A_1 C_1 + \pi^2 \mathcal{T}^2 E_1}. \tag{31}$$

Let us remark that R_S does not depend on J , i.e., R_S does not depend on the inertial term. Hence, R_S coincides with the critical Rayleigh thermal number for the onset of steady convection in the absence of inertia term found in [27]. Furthermore, $\frac{\partial R_S}{\partial \mathcal{T}^2} > 0$, i.e., \mathcal{T}^2 has a stabilizing effect on the onset of steady convection, as one is expected. When $\mathcal{T}^2 = 0$, R_S reduces to

$$(R_S)_{\mathcal{T}^2=0} = \min_{a^2 \in \mathbb{R}^+} \frac{\Lambda^2 A_1}{a^2 C_1}, \tag{32}$$

that is the critical Rayleigh number for the onset of steady convection found in [10] in the absence of rotation. The minimum of R evaluated for $\sigma = 0$ with respect to a^2 is attained at $a^2 = a_s^2$, with a_s^2 being a positive root of a fourth-order degree polynomial:

$$f(x) := A_1 C_1 x^4 + c_1 x^3 + c_2 x^2 + c_3 x - \pi^6 c_4, \tag{33}$$

with c_i constants and

$$c_4 = \left(\pi^2 C_1 + \frac{\pi^2 \mathcal{T}^2 E_1}{A_1} \right) \left(A_1 + \frac{\mathcal{T}^2 B_1}{A_1} + \mathcal{T}^4 \eta^2 \right).$$

Since $\lim_{x \rightarrow \infty} f(x) = \infty$, $f(0) < 0$, a_s^2 exists.

3.2. Oscillatory Convection

In order to determine the critical Rayleigh thermal number for the onset of oscillatory convection, say R_O , then we substitute $\sigma = i\sigma_1$ in (27), with i being the imaginary unit and $\sigma_1 \in \mathbb{R}^+ \setminus \{0\}$. Subsequently, we take the real and imaginary parts of R , require the vanishing of the imaginary part of R , substitute σ_1^2 into the real part of R , and determine the minimum—with respect to $(n, a^2) \in \mathbb{N} \times \mathbb{R}^+$ —of the obtained number. Setting

$$A_2 = \gamma + k_r, \quad B_2 = 2(1 + \gamma)\eta^2, \tag{34}$$

and

$$\begin{aligned} k_{1n} &= \Lambda_n^2 A_1^2 + n^2 \pi^2 \mathcal{T}^2 \Lambda_n B_1 + n^4 \pi^4 \mathcal{T}^4 \eta^2, \quad k_{2n} = \Lambda_n (\Lambda_n A_2^2 + n^2 \pi^2 \mathcal{T}^2 \eta^2), \\ k_{3n} &= \Lambda_n (2\Lambda_n A_1 A_2 + n^2 \pi^2 \mathcal{T}^2 B_2), \quad k_{4n} = \Lambda_n A_1 C_1 + n^2 \pi^2 \mathcal{T}^2 E_1, \\ k_{5n} &= \Lambda_n A_2, \quad k_{6n} = \Lambda_n (A_2 C_1 + A_1) + n^2 \pi^2 \mathcal{T}^2 \eta^2, \end{aligned} \tag{35}$$

one obtains

$$R = \frac{\Lambda_n + i\sigma_1}{a^2} \frac{k_{1n} - \sigma_1^2 J^2 k_{2n} + i\sigma_1 J k_{3n}}{k_{4n} - \sigma_1^2 J^2 k_{5n} + i\sigma_1 J k_{6n}}. \tag{36}$$

Subsequently, one has that $R = R_e(R) + i\sigma_1 Im(R)$ with

$$\begin{aligned} R_e(R) = f_o(a^2) &:= \frac{1}{a^2 [(k_{4n} - \sigma_1^2 J^2 k_{5n})^2 + \sigma_1^2 J^2 k_{6n}^2]} \left\{ \Lambda_n \left[(k_{1n} - \sigma_1^2 J^2 k_{2n})(k_{4n} - \sigma_1^2 J^2 k_{5n}) + \sigma_1^2 J^2 k_{3n} k_{6n} \right] + \right. \\ &\left. - J \sigma_1^2 \left[k_{3n}(k_{4n} - \sigma_1^2 J^2 k_{5n}) - k_{6n}(k_{1n} - \sigma_1^2 J^2 k_{2n}) \right] \right\}. \end{aligned}$$

$$Im(R) = \frac{\{(k_{1n} - \sigma_1^2 J^2 k_{2n})(k_{4n} - \sigma_1^2 J^2 k_{5n}) + \sigma_1^2 J^2 k_{3n} k_{6n} + \Lambda_n J [k_{3n}(k_{4n} - \sigma_1^2 J^2 k_{5n}) - k_{6n}(k_{1n} - \sigma_1^2 J^2 k_{2n})]\}}{a^2 [(k_{4n} - \sigma_1^2 J^2 k_{5n})^2 + \sigma_1^2 J^2 k_{6n}^2]}.$$

The vanishing of the imaginary part of R implies that σ_1^2 has to satisfy

$$k_{2n} k_{5n} J^4 x^2 - J^2 (k_{2n} k_{4n} + k_{1n} k_{5n} - k_{3n} k_{6n} + \Lambda_n J k_{3n} k_{5n} - \Lambda_n J k_{2n} k_{6n}) x + k_{1n} k_{4n} + \Lambda_n J (k_{3n} k_{4n} - k_{1n} k_{6n}) = 0. \tag{37}$$

Subsequently, if

$$k_{2n} k_{4n} + k_{1n} k_{5n} - k_{3n} k_{6n} + \Lambda_n J k_{3n} k_{5n} - \Lambda_n J k_{2n} k_{6n} < 0, \quad k_{1n} k_{4n} + \Lambda_n J (k_{3n} k_{4n} - k_{1n} k_{6n}) > 0, \tag{38}$$

or if

$$(k_{2n} k_{4n} + k_{1n} k_{5n} - k_{3n} k_{6n} + \Lambda_n J k_{3n} k_{5n} - \Lambda_n J k_{2n} k_{6n})^2 - 4k_{2n} k_{5n} [k_{1n} k_{4n} + \Lambda_n J (k_{3n} k_{4n} - k_{1n} k_{6n})] < 0, \tag{39}$$

oscillatory convection can not occur. When the complementary case to (38) and (39) holds, substituting the value of σ_1^2 (positive solution of (37)) in the real part of R and minimizing with respect to $(n, a^2) \in \mathbb{N} \times \mathbb{R}^+$, one obtains the critical Rayleigh thermal number for the onset of oscillatory convection. Numerical simulations show that the minimum—with respect to $n \in \mathbb{N}$ —is attained at $n = 1$ and, hence

$$R_O = \min_{a^2 \in \mathbb{R}^+} f_o(a^2) := \frac{1}{a^2 [(k_4 - \sigma_1^2 J^2 k_5)^2 + \sigma_1^2 J^2 k_6^2]} \left\{ \Lambda \left[(k_1 - \sigma_1^2 J^2 k_2)(k_4 - \sigma_1^2 J^2 k_5) + \sigma_1^2 J^2 k_3 k_6 \right] + \right. \\ \left. - J \sigma_1^2 [k_3(k_4 - \sigma_1^2 J^2 k_5) - k_6(k_1 - \sigma_1^2 J^2 k_2)] \right\} = f_o(a_o^2), \tag{40}$$

with $k_j = k_{1j}$, $j \in \{1, 2, \dots, 6\}$.

4. Numerical Results

Because of the complexity in writing R_O in algebraic closed form, in this section—via Matlab software—we perform some numerical simulations in order to:

- (1) analyze the asymptotic behaviour of R_O with respect to \mathcal{T}^2 and J ; and,
- (2) compare R_S and R_O to establish whether the convection arises through a steady state (stationary convection) or via an oscillatory state (oscillatory convection).

Let us fix $\{\gamma = 0.8, k_r = 1.5, \eta = 0.2\}$ (see [10]) and let \mathcal{T}^2 and J vary separately.

Let us fix $\mathcal{T}^2 = 10$ and let J vary in order to analyze the behaviour of R_O with respect to J . In this case, one has that $a_o^2 = 15.919$, $R_S = 51.9256$ and there exists a threshold $J^* \in (0.31, 0.32)$ for the inertia coefficient, such that R_O exists and convection arises via an oscillatory state (see Table 1). Furthermore, R_O is a decreasing function of J (see Figure 1).

Table 1. Critical threshold of J , from which R_O exists and convection occurs via an oscillatory state in the case $\{\gamma = 0.8, k_r = 1.5, \eta = 0.2, \mathcal{T}^2 = 10\}$.

J	a_o^2	R_O
0	∄	∄
0.25	∄	∄
0.31	∄	∄
0.32	15.3410	51.9150
0.35	14.7812	59.7010
0.4	14.0459	49.0951
0.7	11.9923	44.4657
1	11.2881	42.7649
5	10.3196	40.0417
10	10.2433	39.7591

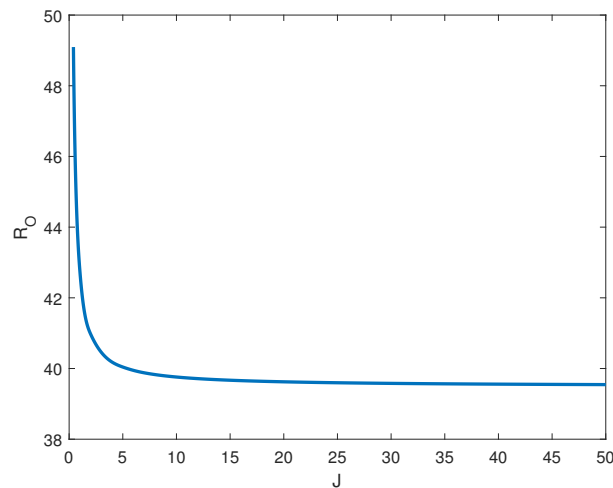


Figure 1. Asymptotic behaviour of R_O with respect to J for $\{\gamma = 0.8; k_r = 1.5, \eta = 0.2, \mathcal{T}^2 = 10\}$.

In Figures 2 and 3, we plot the frequency σ_1^2 of oscillation motions (solution of (37)) with respect to a^2 for different values of J : the graphs show that the existence of $\sigma_1^2(>0)$ and, hence, of R_O is guaranteed for $J > 0.31$.

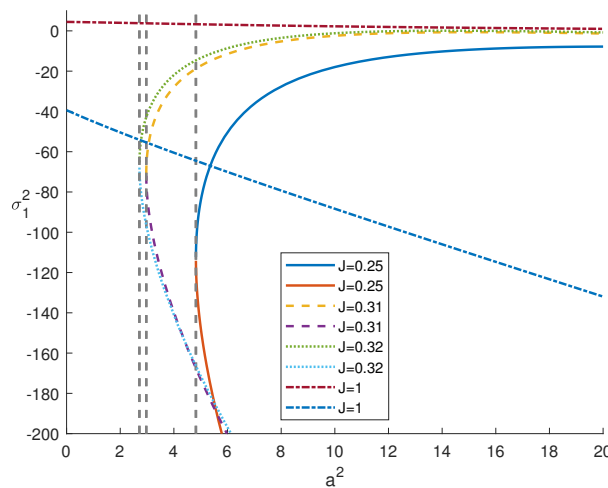


Figure 2. Behaviour of σ_1 versus a^2 .

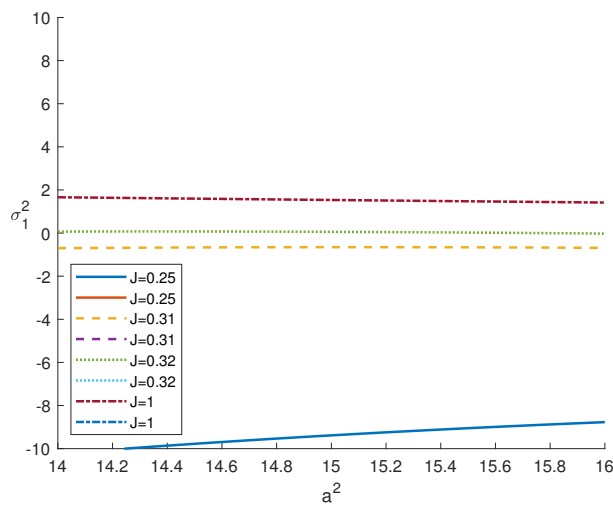


Figure 3. Behaviour of σ_1 versus a^2 .

Let us consider the following parameters set $\{\gamma = 0.8, k_r = 1.5, \eta = 0.2, J = 0.5\}$ and let \mathcal{T}^2 vary in order to analyze the behaviour of R_O with respect to \mathcal{T}^2 . In Table 2 the numerical values of R_O , computed through Matlab software are collected. In particular, we found that: (i) R_O and R_S are increasing functions of \mathcal{T}^2 (see Figure 4); (ii) there exists a threshold $\mathcal{T}^{*2} \in (7.26, 7.27)$ for the Taylor number, such that, if $\mathcal{T}^2 > \mathcal{T}^{*2}$, then the convection arises via an oscillatory state (see Figure 5).

Table 2. Critical threshold of \mathcal{T}^2 from which R_O exists and convection occurs via an oscillatory state in the case $\{\gamma = 0.8, k_r = 1.5, \eta = 0.2, J = 0.5\}$.

\mathcal{T}^2	a_s^2	a_o^2	R_S	R_O
7	15.3031	∅	45.5293	∅
7.07	15.3234	12.5623	45.6906	46.0730
7.1	15.3320	12.5674	45.7596	46.0815
7.2	15.3603	12.5844	45.9885	46.1098
7.26	15.3769	12.5946	46.1253	46.1268
7.27	15.2796	12.5963	46.1480	46.1296
7.3	15.3878	12.6014	46.2162	46.1381
7.5	15.4410	12.6353	46.6677	46.1945
10	15.919	13.0503	51.9256	46.8876
20	16.1538	14.5717	67.9956	49.4695
50	15.2776	18.2109	95.5668	55.9909

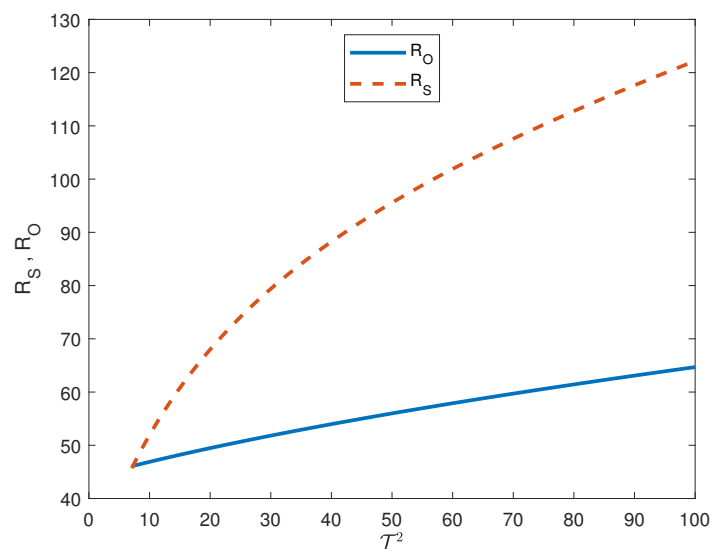


Figure 4. Behaviour of R_S and R_O with respect to \mathcal{T} . The other parameters are set as $\{\gamma = 0.8; k_r = 1.5, \eta = 0.2, J = 0.5\}$.

To compare the asymptotic behaviour of R_O versus R_S to look for the occurrence of steady or oscillatory convection, we have numerically studied some specific cases. For example, on fixing the parameters $\{\gamma = 0.8, k_r = 1.5, \eta = 0.2, J = 1.5\}$ it arises that: for $\mathcal{T}^2 = 30$, convection sets in via an oscillatory state at $R = R_O = 51.8111$ (Figure 5); while, for $\mathcal{T}^2 = 7.1$, there is a switch in the onset of convection that sets in through a steady state $R = R_S = 45.7596$ (Figure 6).

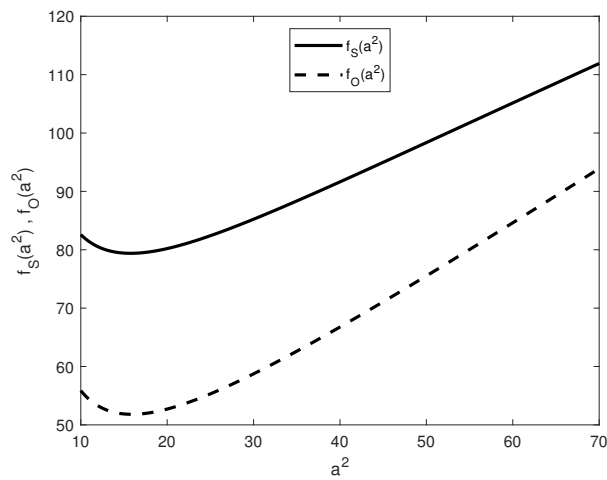


Figure 5. Behaviour of $f_s(a^2)$ and $f_o(a^2)$ for $\gamma = 0.8; k_r = 1.5, \eta = 0.2, J = 1.5$ and $\mathcal{T}^2 = 30$.

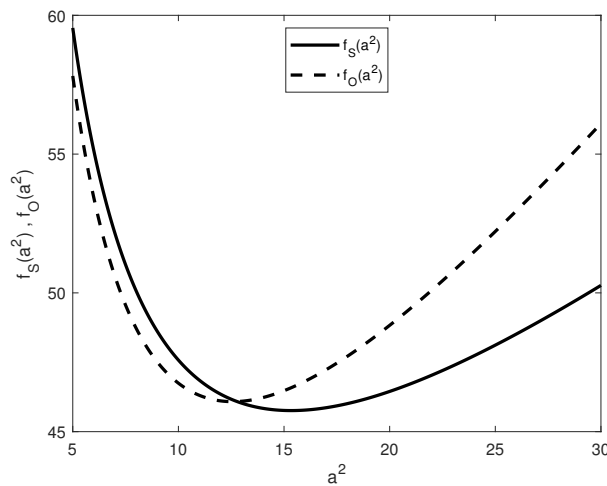


Figure 6. Behaviour of $f_s(a^2)$ and $f_o(a^2)$ for $\gamma = 0.8; k_r = 1.5, \eta = 0.2, J = 1.5$ and $\mathcal{T}^2 = 7.1$.

The asymptotic behaviour of $f_o(a^2)$ with respect to \mathcal{T}^2 and J is shown in Figures 7 and 8, respectively. In particular, Figure 7 shows that, for $\{\gamma = 0.8, k_r = 1.5, \eta = 0.2, J = 10\}$, R_O increases with \mathcal{T}^2 and, hence, as one is expected, rotation has a stabilizing effect on the onset of convection. Figure 8 shows that, for $\{\gamma = 0.8, k_r = 1.5, \eta = 0.2, \mathcal{T}^2 = 10\}$, R_O decreases with J and, hence, J has a destabilizing effect on the onset of oscillatory convection.

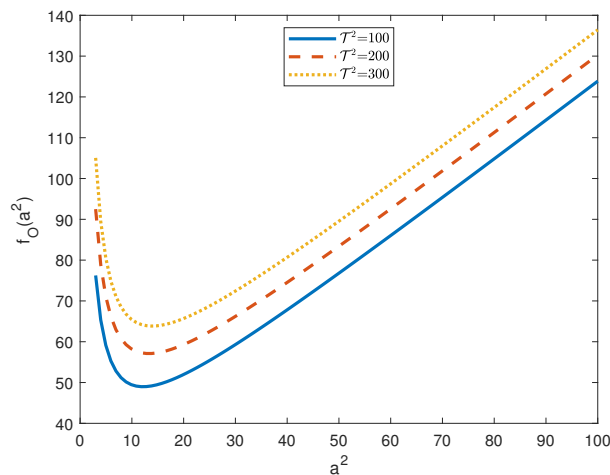


Figure 7. Plot of $f_o(a^2)$ for $\gamma = 0.8, k_r = 1.5, \eta = 0.2, J = 10$.

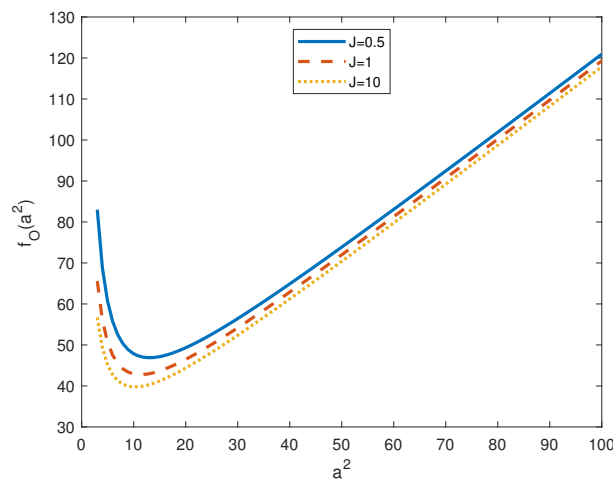


Figure 8. Plot of $f_0(a^2)$ for $\gamma = 0.8, k_r = 1.5, \eta = 0.2, \mathcal{T}^2 = 10$.

Table 3 displays the numerical values of a_s^2, a_o^2, R_S and R_O of the previous examples.

Table 3. Onset of steady or oscillatory convection.

γ	k_r	η	\mathcal{T}^2	J	a_s^2	a_o^2	R_S	R_O	CONVECTION
10	7	2	30	1.3	22.74	15.78	198.64	202.89	STEADY
10	7	2	100	1.3	37.07	21.08	437.66	289.54	OSCILLATORY
0.8	1.5	0.2	300	10	19.25	13.92	193.25	63.84	OSCILLATORY
0.8	0.5	0.2	100	1	21.27	\nexists	120.07	\nexists	STEADY
0.8	0.5	0.2	100	1.5	21.27	17.10	120.07	44.72	OSCILLATORY

On summarizing we have found numerically some thresholds \mathcal{T}_c^2 and J_c such that:

- (i) if $\mathcal{T}^2 < \mathcal{T}_c^2$ or if $\{\mathcal{T}^2 > \mathcal{T}_c^2, J < J_c\}$, then convection can only arise via a steady state;
- (ii) if $\{\mathcal{T}^2 > \mathcal{T}_c^2, J > J_c\}$, convection can only arise via an oscillatory state.

5. Conclusions

In this paper, the onset of thermal convection in a horizontal bidispersive porous layer, uniformly heated from below and rotating about a vertical axis, is analyzed in the presence of inertial effects.

The critical Rayleigh number for the onset of steady convection, R_S , has been found in algebraic closed form and it has been found that:

- R_S does not depend on the acceleration coefficient, i.e., inertial effects do not affect R_S ;
- R_S increases with the Taylor number, i.e., \mathcal{T}^2 has—as one is expected—a stabilizing effect on the onset of steady convection; and,
- R_S reduces to the critical Rayleigh number for the onset of steady convection found in [27] in the absence of inertia and to the critical Rayleigh number for the onset of steady convection found in [10] in the absence of rotation.

Moreover, due to the complexity in evaluating exactly the threshold for the onset of oscillatory convection R_O , we have performed some numerical simulations through Matlab software in order to analyze the influence of rotation and acceleration coefficient on R_O . In particular, we have found that:

- R_O is a decreasing function of J and there exists a threshold $J^* \in (0.31, 0.32)$ for the inertia coefficient, such that R_O exists and convection arises via an oscillatory state; and,
- R_O is an increasing functions of \mathcal{T}^2 and there exists a threshold \mathcal{T}^{*2} for the Taylor number, such that, for $\mathcal{T}^2 > \mathcal{T}^{*2}$, the convection arises via an oscillatory state.

Finally, we have compared R_S and R_O to establish whether the convection arises through a steady state (stationary convection) or via an oscillatory state (Hopf bifurcation).

Author Contributions: The authors (F.C. and R.D.L.) conceived the mathematical model, proved the mathematical results and wrote the paper together. All authors have read and agreed to the published version of the manuscript.

Funding: This research received no external funding.

Acknowledgments: The paper has been performed under the auspices of GNFM of INdAM. The Authors should like to thank the anonymous referees for suggestions which have led to improvements in the manuscript.

Conflicts of Interest: The authors declare no conflict of interest.

References

1. Capone, F.; Gentile, M.; Hill, A.A. Convection problems in anisotropic porous media with nonhomogeneous porosity and thermal diffusivity. *Acta Appl. Math.* **2012**, *122*, 85–91. [[CrossRef](#)]
2. Capone, F.; Rionero, S. Porous MHD convection: Stabilizing effect of magnetic field and bifurcation analysis. *Ricerche Mat.* **2016**, *65*, 163–186. [[CrossRef](#)]
3. Straughan, B. *Stability and Wave Motion in Porous Media. Applied Mathematical Sciences*; Springer: Berlin, Germany, 2008; Volume 165.
4. Chen, Z.Q.; Cheng, P.; Hsu, C.T. A theoretical and experimental study on stagnant thermal conductivity of bi-dispersed porous media. *Int. Commun. Heat Mass Transf.* **2000**, *27*, 601–610. [[CrossRef](#)]
5. Chen, Z.Q.; Cheng, P.; Zhao, T.S. An experimental study of two phase flow and boiling heat transfer in bi-disperse porous channels. *Int. Commun. Heat Mass Transf.* **2000**, *27*, 293–302. [[CrossRef](#)]
6. Nield, D.A.; Kuznetsov, A.V. The onset of convection in a bidisperse porous medium. *Int. J. Heat Mass Transf.* **2006**, *49*, 3068–3074. [[CrossRef](#)]
7. Lin, F.C.; Liu, B.H.; Huang, C.T.; Chen, Y.M. Evaporative heat transfer model of a loop heat pipe with bidisperse wick structure. *Int. J. Heat Mass Transf.* **2011**, *54*, 4621–4629 [[CrossRef](#)]
8. Borja, R.L.; Liu, X.; White, J.A. Multiphysics hillslope processes triggering landslides. *Acta Geotech.* **2012**, *7*, 261–269. [[CrossRef](#)]
9. Straughan, B. Convection with Local Thermal Non-Equilibrium and Microfluidic Effects. In *Advances in Mechanics and Mathematics*; Springer: Cham, Switzerland, 2015; Volume 32.
10. Straughan, B. Effect of inertia on double diffusive bidispersive convection. *Int. J. Heat Mass Transf.* **2019**, *129*, 389–396. [[CrossRef](#)]
11. Nield, D.A.; Bejan, A. *Convection in Porous Media*, 5th ed.; Springer: Cham, Switzerland, 2017.
12. Rees, D.A.S. The effect of inertia on free convection from a horizontal surface embedded in a porous medium. *Int. J. Heat Mass Transf.* **1996**, *39*, 3425–3430. [[CrossRef](#)]
13. Rees, D.A.S. The effect of inertia on the onset of mixed convection in a porous layer heated from below. *Int. Comm. Heat Mass Transf.* **1997**, *24*, 277–283. [[CrossRef](#)]
14. Rabbani, S.; Abderrahmane, H.; Sassi, M. Inertial Effects on Dynamics of Immiscible Viscous Fingering in Homogenous Porous Media. *Fluids* **2019**, *4*, 79. [[CrossRef](#)]
15. Capone, F.; De Luca, R. Porous MHD convection: Effect of Vadasz inertia term. *Transp. Porous Med.* **2017**, *118*, 519–536. [[CrossRef](#)]
16. Capone, F.; De Luca, R.; Vitiello, M. Double-diffusive Soret convection phenomenon in porous media: Effect of Vadasz inertia term. *Ricerche Mat.* **2019**, *68*, 581–595. [[CrossRef](#)]
17. Capone, F.; Rionero, S. Inertia effect on the onset of convection in rotating porous layers via the “auxiliary system method”. *Int. J. Non-Linear Mech.* **2013**, *57*, 193–200. [[CrossRef](#)]
18. Vadasz, P. Coriolis effect on gravity-driven convection in a rotating porous layer heated from below. *J. Fluid Mech.* **1998**, *376*, 351–375. [[CrossRef](#)]
19. Dogdson, E.; Rees, D.A.S. The onset of Prandtl-Darcy-Prats convection in a horizontal porous layer. *Transp. Porous Med.* **2013**, *99*, 175–189.
20. Capone, F.; Gentile, M. Sharp stability results in LTNE rotating anisotropic porous layer. *Int. J. Therm. Sci.* **2019**, *134*, 661–664. [[CrossRef](#)]
21. De Luca, R.; Rionero, S. Steady and oscillatory convection in rotating fluid layers heated and salted from below. *Int. J. Non-Linear Mech.* **2016**, *78*, 121–130. [[CrossRef](#)]

22. Capone, F.; De Luca, R. On the stability-instability of vertical throughflows in double diffusive mixtures saturating rotating porous layers with large pores. *Ric. Mat.* **2014**, *63*, 119–148. [[CrossRef](#)]
23. De Luca, R.; Rionero, S. Dynamic of rotating fluid layers: L^2 -absorbing sets and onset of convection. *Acta Mech.* **2017**, *228*, 4025–4037. [[CrossRef](#)]
24. Vadasz, P. *Fluid Flow and Heat Transfer in Rotating Porous Media*; Springer Briefs in Thermal Engineering and Applied Science (eBook); Springer International Publishing: New York, NY, USA, 2016.
25. Vadasz, P. Instability and convection in rotating porous media: A review. *Fluids* **2019**, *4*, 1–31. [[CrossRef](#)]
26. Falsaperla, P.; Mulone, G.; Straughan, B. Inertia effects on rotating porous convection. *Int. J. Heat Mass Transf.* **2011**, *54*, 1352–1359. [[CrossRef](#)]
27. Capone, R.F.; De Luca, M. Gentile, Coriolis effect on thermal convection in a rotating bidispersive porous layer. *Proc. R. Soc. Lond. A* **2020**. [[CrossRef](#)]
28. Falsaperla, P.; Mulone, G.; Straughan, B. Bidispersive inclined convection. *Proc. R. Soc. A* **2016**, *472*, 20160480. [[CrossRef](#)] [[PubMed](#)]



© 2020 by the authors. Licensee MDPI, Basel, Switzerland. This article is an open access article distributed under the terms and conditions of the Creative Commons Attribution (CC BY) license (<http://creativecommons.org/licenses/by/4.0/>).